We are IntechOpen, the world's leading publisher of Open Access books Built by scientists, for scientists

4,800
Open access books available

122,000
International authors and editors

135M
Downloads

Our authors are among the

154
Countries delivered to

TOP 1%
most cited scientists

12.2%
Contributors from top 500 universities

CLARIVATE ANALYTICS BOOK CITATION INDEX INDEXED

WEB OF SCIENCE™

Selection of our books indexed in the Book Citation Index in Web of Science™ Core Collection (BKCI)

Interested in publishing with us?
Contact book.department@intechopen.com

Numbers displayed above are based on latest data collected.
For more information visit www.intechopen.com

Chapter 2

Texture, Microstructure, and Mechanical Properties of Calcium-Containing Flame-Resistant Magnesium Alloy Sheets Produced by Twin-Roll Casting and Sequential Warm Rolling

Masafumi Noda, Tomomi Ito, Yoshio Gonda,
Hisashi Mori and Kunio Funami

Additional information is available at the end of the chapter

http://dx.doi.org/10.5772/58940

1. Introduction

Magnesium (Mg) alloys are attracting attention as metallic materials of the next generation because of their good specific strength, specific rigidity, earthquake resistance, and machinability, as well as the abundance of resources available for their production [1]. Because of their lightness, Mg alloys are expected to be suitable materials for replacing aluminum alloys in automobiles and in rail and aerospace transportation devices [2,3]. Research has been performed on improving the mechanical properties, corrosion resistance, and workability of Mg alloys [4,5]. Hot working is required in plastic forming of Mg alloys because of their crystal structure [6]. Problems associated with Mg alloys include their high production costs, their high flammability, and the marked effects of additive elements on the various properties of the alloys. Most structural parts currently manufactured from Mg alloys are die cast, Thixomolded [7,8], semicontinuously cast, or gravity cast [8,9], or they are forged from such materials. The amount of wrought materials that are used is low, representing less than 10% of all Mg alloys that are used [10]. Recently, the problems associated with Mg alloys have been resolved by increasing their strength [11–13] and by improving their creep properties [14], heat resistance [15], and formability [16,17] by adding trace amounts of various elements [18,19], by age-hardening effects [20], by crystal-grain refinement [21,22], and by texture control [23,24]. However, there is still a need for incombustible or noncombustible Mg alloys [25-27] for use in structural or construction components. Flame-resistant and noncombustible Mg alloys have recently been developed by adding Ca to Mg alloys [25–28], and these materials

have received flame-resistance and noncombustion certifications in the rail, aerospace, and construction sectors.

There are many choices of starting material for manufacturing sheet products, and use of twin-roll cast (TRC) materials [29–32] should be examined if production costs are a consideration. However, TRC materials have a number of problems, such as solidifying segregation at the slab thickness center, intrusion of inclusions during casting, and restrictions on casting conditions, such as the casting length, liquid pressure, rolling speed, and quenching capacity [30–32]. Moreover, most generic TRC materials in use are Al alloys or AZ-type Mg alloys that do not preferentially form intermetallic compounds [30–33]. TRC materials described in the literature are subjected to a short TRC process, so that the melt is exposed to the air for only a short time and there is no blackening of the sheet surface through ignition during casting. There is a report that the manufacture of a sheet material from AZ-type Mg alloys can be problematic unless the twin-rolling speed is unusually slow at casting temperatures exceeding 620 °C [34], but there has been no discussion on the effects of the metal texture and the role of plastic deformation after casting. In addition, there has been insufficient discussion on the effect of melt purification before TRC casting and on the role of additive elements on twin-roll casting conditions and the internal texture. Furthermore, there is no report of any comparison with semicontinuous casting in the manufacture of sheet material. We have therefore describe our investigations on the effects of melt purification during melting before TRC on the production of sheet materials, as well as the microstructure and mechanical properties of twin-roll cast Ca-containing flame-resistant Mg alloys; we also provide an analysis of the effects on the cast sheets and their durability caused by precipitation of intermetallic compounds formed through addition of Ca.

2. Experimental procedures

To investigate the effects of the alloy composition on materials produced under TRC conditions, samples of AZ61 alloy and of AZX611 and AZX612 alloys containing 1 or 2 mass% of added Ca, respectively, were prepared from AM60B Mg and Mg–30%Ca master alloy, pure Al ingots (99.7%), and pure Zn ingots (99.9%). The metals were weighted to the required stoichiometry, placed in a steel crucible, and melted by heating to 700 °C in an electric furnace. Melting was carried out under an argon atmosphere, and argon gas was bubbled through the melt for 20 min. The slug was removed and immediately tapped when the melt temperature reached 660 °C. To prevent combustion of the weighed metals, the melt was isolated from the atmosphere by placing a steel lid on the crucible. The conditions for twin-roll casting were as follows. The speed of both the upper and lower rolls was 20–25 m min^{-1}, and the roll gap was 2 – 3 mm. The rolls used were metal rolls 300 mm wide with a diameter of 200 mm. The surface of the roll was heated to a temperature of more than 100 °C before twin-roll casting prior to decreasing the cooling rate. Grooves were cut into the rolls to facilitate peeling of sheets during twin-roll casting. Figure 1 is a schematic showing the twin-roll casting process. After twin-roll casting, the sheets were left to cool to room temperature and then subjected to strip processing. Sheets measuring 150 mm in width by 200 mm in length were cut from the TRC material for

http://dx.doi.org/10.5772/58940

strip processing, with the width direction of the cut sheets aligned in the casting direction. Strip processing was performed by using a two-high rolling mill with 300 mm diameter rolls. The thickness of the original sheet was reduced by 65% in one pass: the roll surface temperature was 245 °C, the workpiece was heated for 10 min at 200–400 °C, the roll speed during processing was 5–25 m min^{-1}, and the workpiece was cooled with water after the strip processing. Tensile-test specimens with a gauge length of 30 mm and a width of 4 mm were prepared from the strip-processed materials, and tensile tests were carried out in air at an initial strain rate of 1.3 × 10^{-3} s^{-1}. The microstructures of the TRC materials and the strip-processed materials were examined by optical microscopy (OM), and scanning electron microscopy (SEM), and the crystal orientation was analyzed by using electron backscattered diffraction (EBSD).

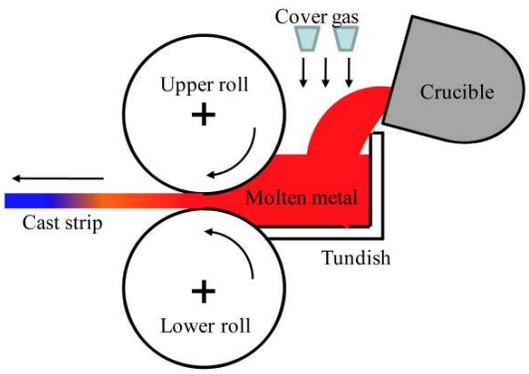

Figure 1. Schematic of a twin-roll caster for strips.

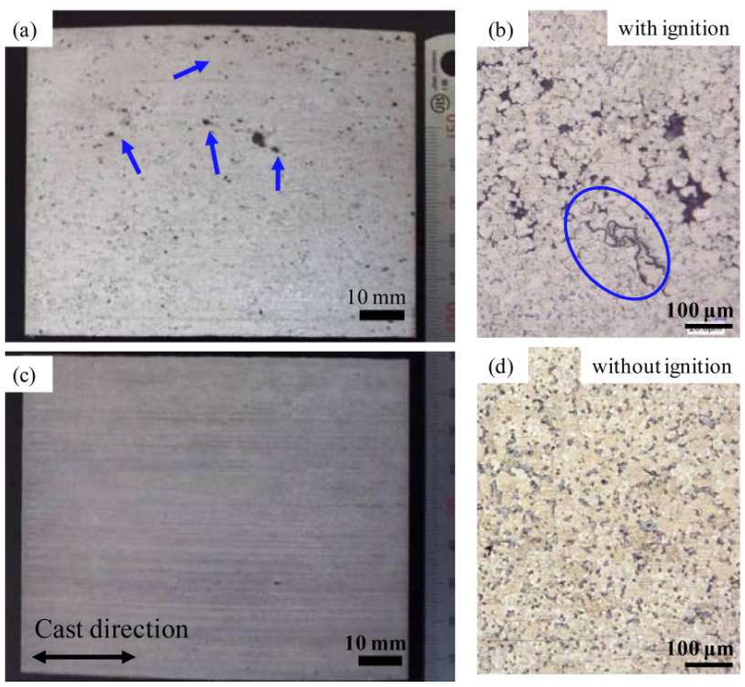

Figure 2. Surface of cast material plate with ignition (a) and without ignition (c), and optical micrographs of twin-roll cast material with ignition (b) and without ignition (d).

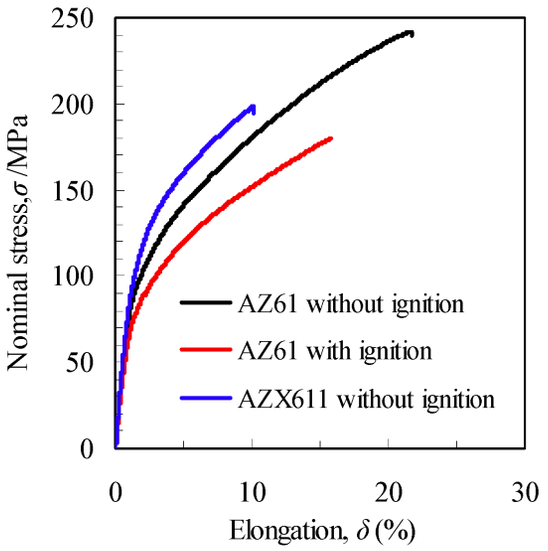

Figure 3. Nominal stress–strain curves for AZ61 and AZX611 twin-roll cast materials.

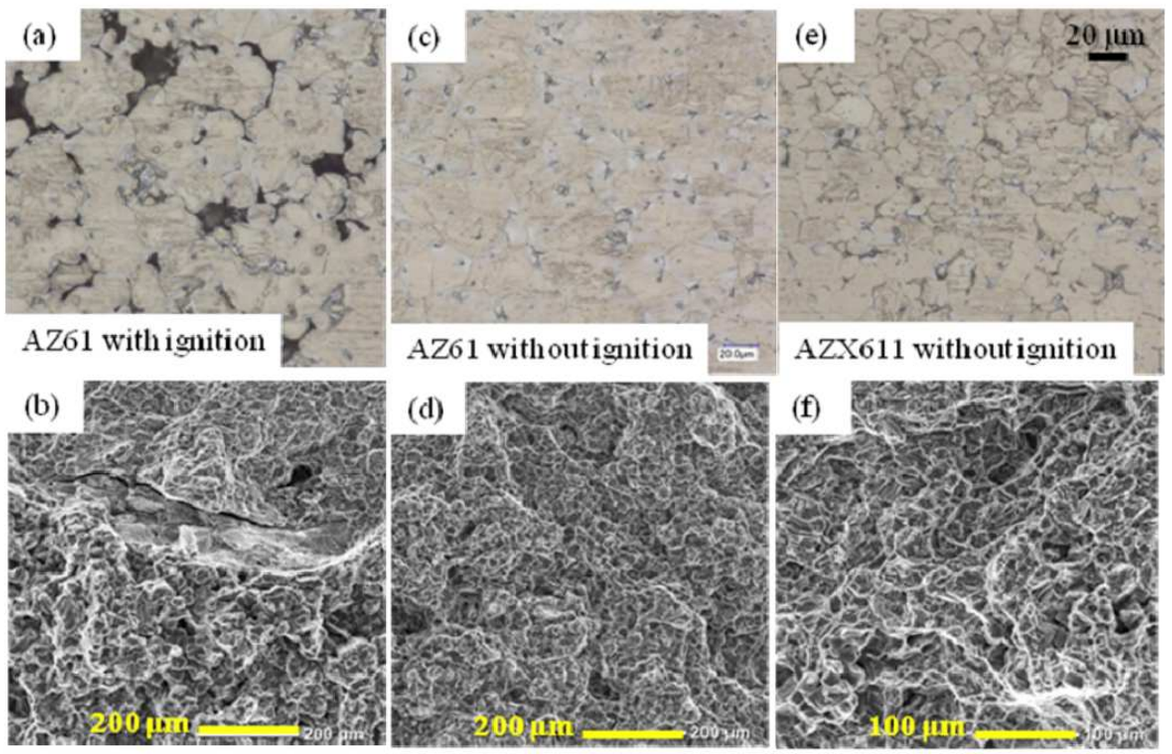

Figure 4. Cross-sectional optical micrographs [(a), (c), and (e)] and SEM micrographs of fracture surfaces [(b), (d), and (f)] of AZ61 [(a)–(d)] and AZX611 [(e) and (f)] twin-roll cast materials with ignition during heating [(a) and (b)] and without ignition during heating [(c)–(f)].

http://dx.doi.org/10.5772/58940

3. Results and discussions

3.1. The twin-roll casting process and microstructure

Figure 2(a)–(d) show external views and internal microstructures of sheets subjected to melting in an argon (Ar) atmosphere, bubbling with argon gas, and twin-roll casting. Slight combustion caused oxides to form in the melt and increased the frequency of intrusion of oxides and impurities. Figure 2(a) and 2(b) show the presence of black spots on the surface of the sheet and the inclusion of oxides and impurities in the microstructure. The nominal stress–strain curves of the TRC AZ61 and AZX611 alloys are shown in Figure 3, and the vertical cross-sections and fracture surface microstructure are shown in Figures 4(a)–(f). Two types of AZ61 alloys are shown in Figure 4(a)–(d), one in which combustion occurred during melting and one in which it did not occur. The AZX611 alloy melt did not undergo combustion during TRC. When no combustion occurred during melting, the yield stress (YS) was 116 MPa, the ultimate tensile strength (UTS) was 239 MPa, and the elongation was 19% [Figures 4(a) and 4(b)], whereas when combustion occurred, the YS was 82 MPa, the UTS was 180 MPa, and the elongation was 13% [Figures 4(c) and 4(d)]. Intrusion of inclusions and oxides caused early fracture without sufficient plastic deformation [35], and the tensile properties were stable when melts that had not undergone combustion were used. Figure 4 shows that intrusion of oxides caused by combustion results in propagation of cracks, formation of voids, and the appearance of partial brittle fracture. Most of the brittle fracture occurs near the surface of the TRC material, implying that the solidification rate is faster at the surface of the sheet than in its interior, that internal latent heat causes coarsening of the microstructure, and that crack propagation along grain boundaries is initiated from internal voids, resulting ultimately in fracture. In contrast, AZ61 alloy that had not undergone combustion showed a standard ductile fracture surface. In AZX611 alloy containing 1 mass% of Ca, no intrusions of oxides were found and the YS (139 MPa) was higher than that of AZ61 alloy; however, the elongation was only about 8%. Because Al–Ca compounds form at grain boundaries, as shown in Figures 4(e) and 4(f), the reason for early fracture compared with AZ61 alloy is likely to be inhibition of plastic deformation by Al–Ca compounds.

Figure 5 shows the SM and OM microstructures of TRC AZ61 and AZX611 alloys for the case where the roll was at room temperature, the melt temperature was 660 °C, and the roll speed was 25 m min^{-1}. Figures 5(a) and 5(b) show that no cracks were present at the surface of the TRC material in the AZ61 alloy, but that cracks appeared at grooves in the AZX611 alloy. Al–Ca compounds are known to form in AZX611 alloy [3,11]. Figures 5(c) and 5(d) show the OM microstructure after removal of 0.1 mm of material from the sheet surface by mechanical polishing, and they show that Al–Ca compounds formed near cracks in the AZX611 alloy. There was considerable segregation near the surface in the processed sheets shown in Figure 5(d), suggesting that the cooling rate in twin-roll casting is too rapid for alloy systems that form compounds.

Figure 6 shows an example in which Al–Ca compounds segregate at the surface of the TRC material. Because Al–Ca compounds form where the quenching capacity is largest, the rate of solidification of the melt in the twin-roll casting process was reduced by adjusting the

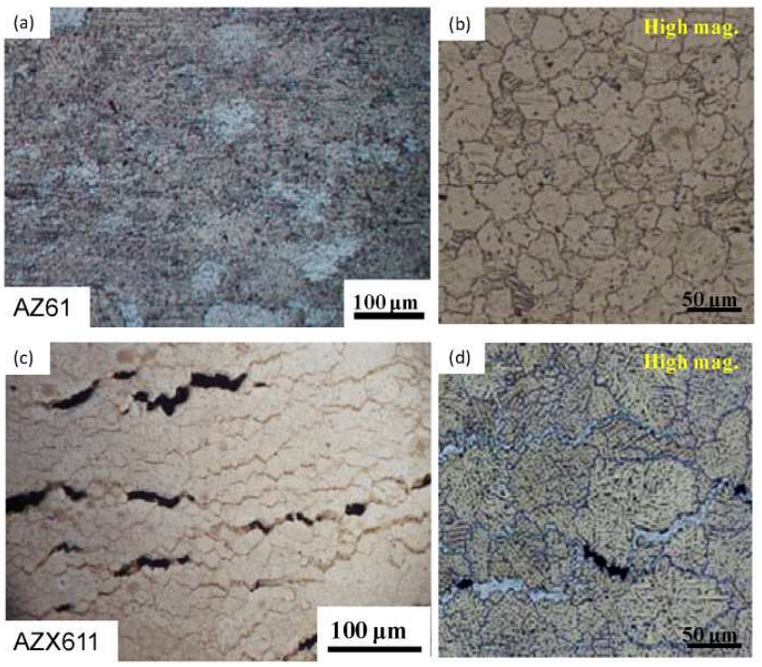

Figure 5. Optical micrographs of the surfaces of twin-roll cast strips of AZ61 [(a), (b)] and AZX611 [(c), (d)].

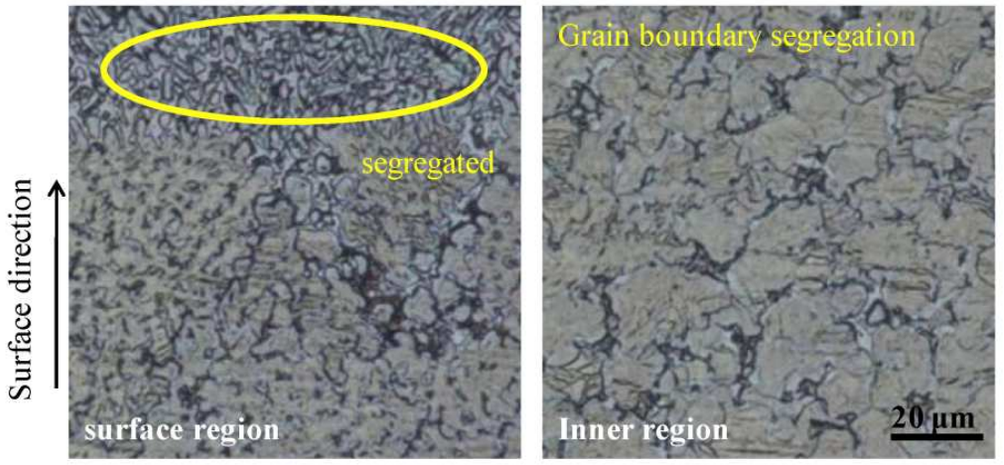

Figure 6. Example showing the segregation of Al–Ca compounds in a rapidly cooled region of twin-roll cast material.

temperature of the roll surface to 100 °C and decreasing the roll speed to 20 m min^{-1}. Optical micrographs showing the microstructure of the surface of the resulting sheet and of a cross section perpendicular to the surface are presented in Figure 7. No cracks were found and no segregation of Al–Ca compounds was observed in the prepared sheet. In this case, the sheet temperature immediately after twin-roll casting was 560 °C. By reducing the cooling rate from that of fast solidification at over 100 °C s^{-1}, characteristic of twin-roll casting [29,33], to around 50 °C s^{-1}, samples of TRC Mg alloy material 300 mm wide by 5 m long that form intermetallic compounds can be prepared, as shown in Figure 8.

http://dx.doi.org/10.5772/58940

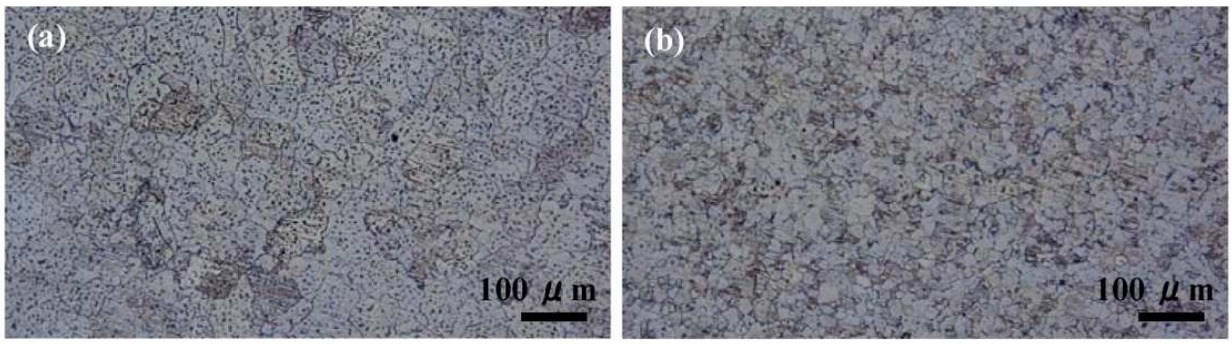

Figure 7. Optical micrographs of AZX611 twin-roll cast material solidified at a lower rate (rise to roll-surface temperature, lower roll-mill speed). Observations were made from the direction of the surface (a) and in the perpendicular direction (b).

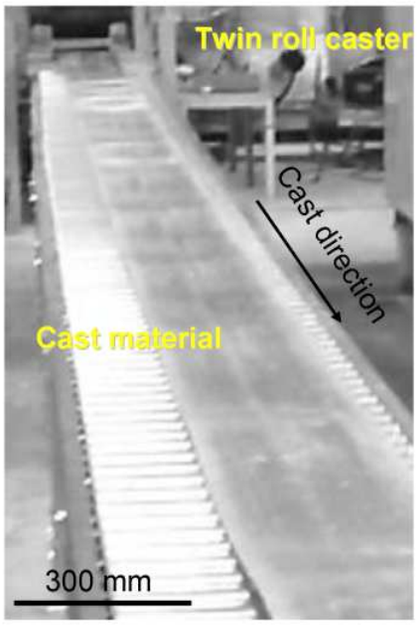

Figure 8. Twin-roll cast AZX611 Mg strip of thickness 2.5 mm and width 300 mm fabricated by using a pilot-plant twin-roll casting machine.

3.2. Comparisons of the texture, microstructure, and mechanical properties of twin-roll cast material with those of normally cast material

The thermal conductivities of AZ61, AZX611, and AZX612 alloy are 63.6, 70.2, and 77.2 W / mK, respectively; therefore, the thermal conductivity increases with addition of Ca. This means that the optimal twin-roll casting conditions will be different for each alloy and, for each sheet, the surface and the interior will have different microstructures. Figure 9 shows the surface and interior OM microstructures of AZ61 and AZX611 TRC alloys. The grain size at the surface of the TRC material is about 2.5 times larger than that in the interior. The surface microstructure consists of coarse grains 70–100 μm in size or dendrites, whereas the interior consists of refined

equiaxial grains 25–40 μm in size. The region with refined equiaxial grains account for two-thirds of the thickness of the sheet.

The inverse pole figure (IPF) map and the pole figure (PF) map obtained by EBSD analysis of the surface and interior of TRC AZX611 alloy are shown in Figure 10. TRC material does not show any specific crystal orientation in either the surface or the interior, regardless of grain size. As shown in Figure 9(a), the texture orientation is high (10.9) because of the large size of the crystal grains compared with the visual area for measurement. The microstructure orientation of the interior texture is 3.8, indicating a random orientation. One noteworthy point is that the OM microstructure and IPF map suggest that a grain boundary forms between the refined-grain region and coarse-grain region. However, measurement of the crystal orientation between adjacent grains showed that coarse grains adjacent to regions of refined grains are in fact agglomerates of refined subgrains. This means that differences between the surface and interior microstructure can be reduced by optimizing the twin-roll casting method or by a cooling and homogenization processes after twin-roll casting. No cracks at interfaces or grain boundaries were found in either the coarse-grain region or the refined-grain region.

Table 1 lists the average grain sizes at the surfaces and in the interiors of AZ61, AZX611, and AZX612 TRC alloys, as well as the proportion of compound formation and the hardness. These measurements were performed by using 3 mm thick TRC sheets. As the Ca content increases, the crystal grain size becomes smaller, the area ratio of intermetallic compounds increases, and the hardness increases. Figure 11 shows the OM structure and the IPF and FP maps for AZX611 alloy semicontinuously cast at a cooling rate of 25 °C s^{-1}. The average grain size of the standard gravity-cast material is around 600–800 μm [11]. This can be refined to about 100 μm by increasing the cooling rate, thereby making possible refined dispersion of Al–Ca compounds in the Mg phase [35]. Here, the texture orientation is 10.9 and a dendrite microstructure is present in the crystal texture, showing the same trends as the microstructure of the surface of TRC material. The YS and UTS of semicontinuously cast material have been reported to be 90 MPa and 155 MPa, respectively, and the elongation is 5%. The elongation is lower than that found in tensile tests on TRC AZX611 material, although the tensile behavior is similar. Therefore, large changes in single uniaxial tensile tests were not observed when the cooling rate exceeded a certain value and the average grain size after casting was less than 100 μm, Addition of Ca causes minute cracks to form more easily, as mentioned before, and similar results are found in semicontinuously cast material. On the other hand, as Al–Ca compounds are smaller and undergo refined dispersion in the Mg phase in TRC material, as shown in Figures 10 and 11, the rolling reduction per pass can be large in the strip-processing technique described later. The results agree with the maximum rolling reduction curve for extruded AZX311 determined by Noda *et al.* [11] The use of extruded materials or TRC materials instead of cast materials with a dendrite microstructure and/or coarse grains results in good strip-processing performance as a result of random crystal orientation, formation of a refined texture, and refined dispersion of Al–Ca compounds.

http://dx.doi.org/10.5772/58940

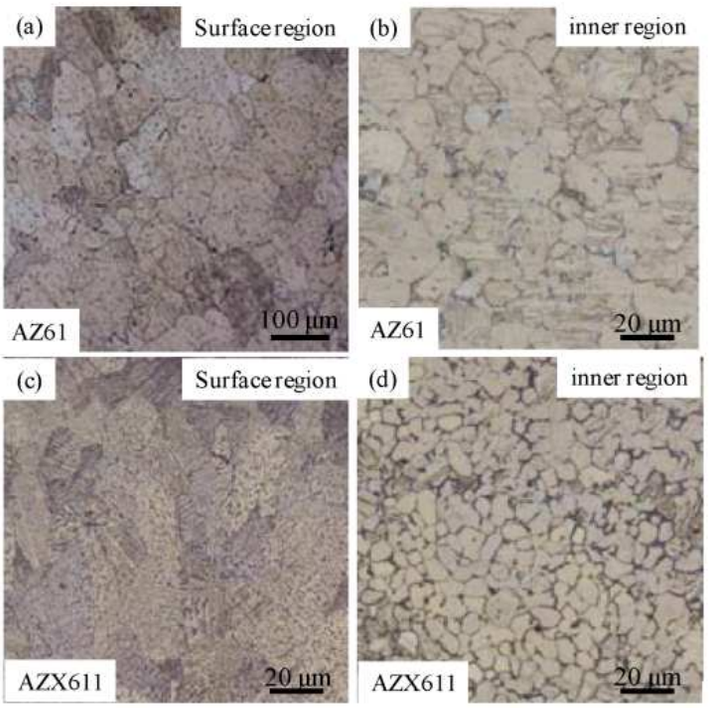

Figure 9. Optical micrographs of twin-roll cast strips of AZ61 [(a) and (b)] and AZX611 [(c) and (d)] showing the surfaces of the strips [(a) and (c)] and the interiors of the strips [(b) and (d)].

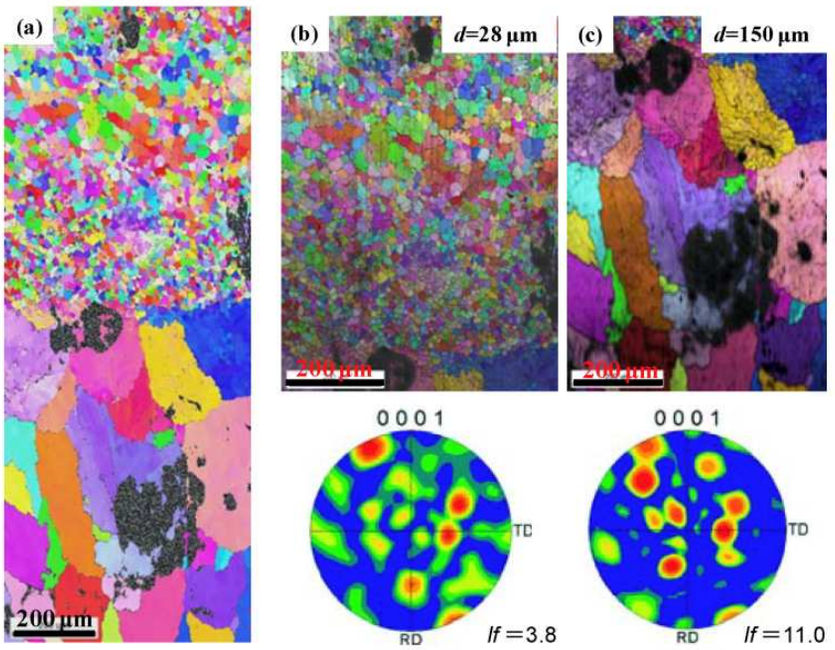

Figure 10. Inverse pole figure (IPF) maps and pole figure (PF) maps of AZX611 twin-roll cast material. The intensity of texture is indicated in the PF maps. Figures (b) and (c) were cropped from the IPF map; (b) shows the surface region and (c) shows the interior.

Material	Vickers hardness (HV)	Mean grain size Surface / Inner region	Thermal conductivity (W/mK)	Area frequency of compounds (%)
AZ61	64	93 μm / 37 μm	63.6	0.8
AZX611	66	70 μm / 24 μm	70.2	7.1
AZX612	68	73 μm / 17 μm	77.2	18.1

Table 1. Grain size, Vickers hardness, and area frequency of compounds for various twin-roll cast materials.

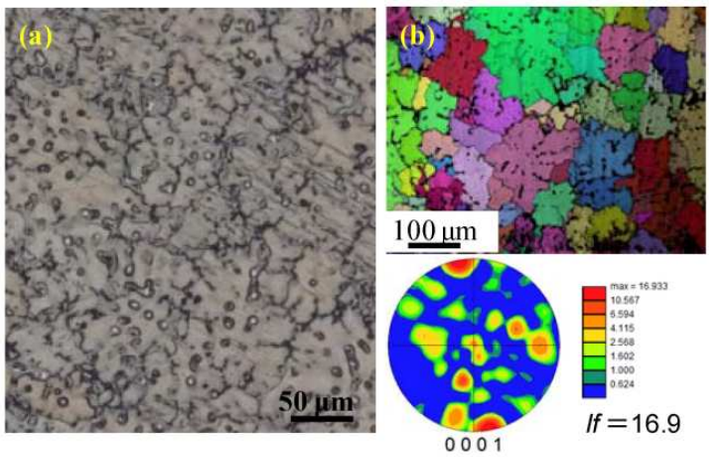

Figure 11. Optical micrograph and IPF and PF maps of AZX611 antigravity suction-cast material cooled at 25 °C s^{-1}. The intensity of texture is indicated in the PF map.

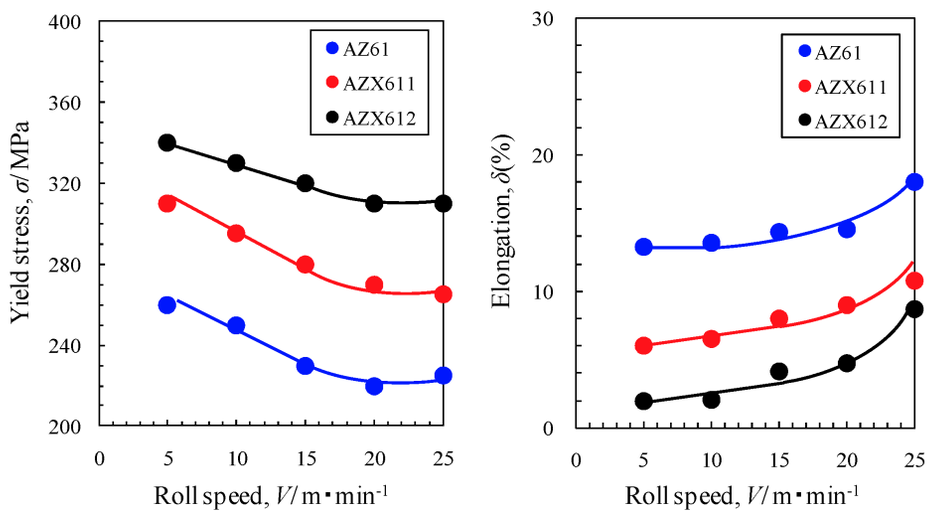

Figure 12. Relationship between tensile properties and roll-mill speed for AZ61, AZX611, and AZX612 twin-roll cast materials subjected to a single-pass rolling process.

http://dx.doi.org/10.5772/58940

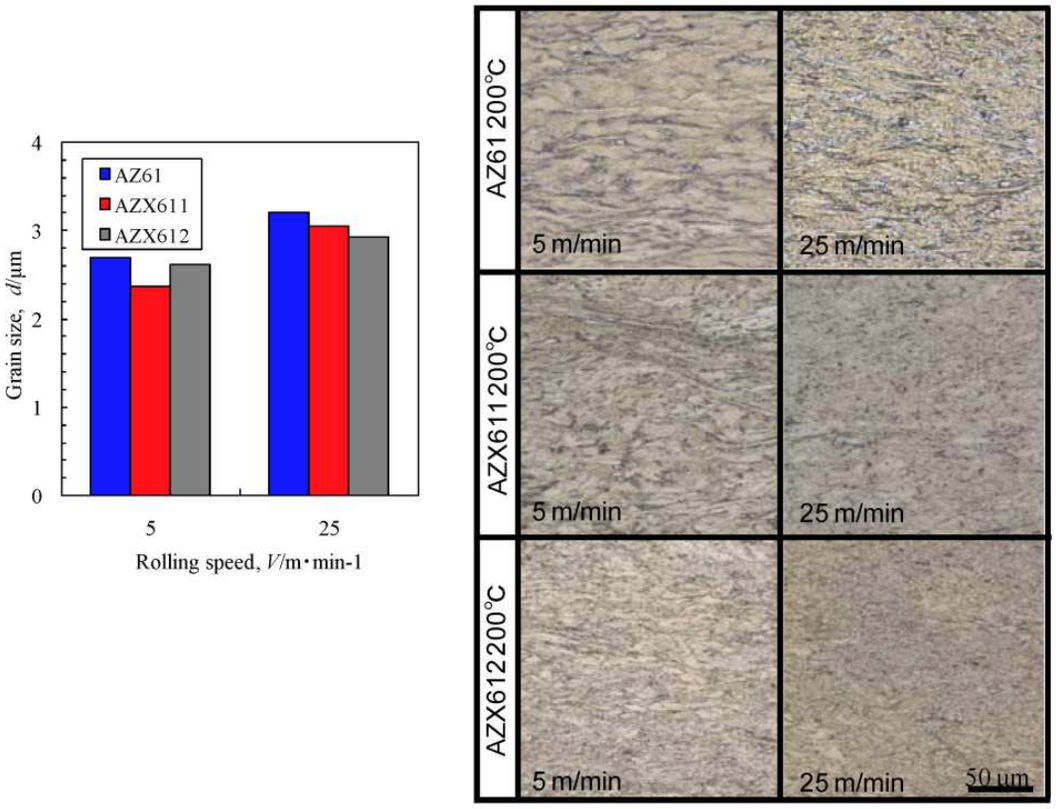

Figure 13. (a) Relationship between the grain size and the annealing temperature for single-pass rolled samples of AZ61, AZX611, AZX 612; and (b) optical micrographs of AZ61, AZX611, and AZX612 materials subjected to single-pass rolling at a sample temperature of 200 °C. The roll-mill speeds are indicated in the optical micrographs.

3.3. Mechanical properties and microstructures of rolled materials

Figure 12 shows the tensile properties of TRC AZ61, AZX611, and AZX612 alloys subjected to strip processing with large one-pass rolling reductions with a strip roll-surface temperature of 245 °C, a specimen temperature of 200 °C, and various roll speeds. The OM microstructures and recrystallized grain sizes are given in Figure 13. The rolling reduction was 65% of the original thickness. According to Figure 12, the YS of AZ61alloy decreased monotonously from 260 MPa to 230 MPa, and that of AZX611 decreased monotonously from 310 MPa to 270 MPa when the strip processing speed was increased to 15 m min^{-1}. Increasing the roll speed further to 25 m min^{-1} resulted in a decrease in the YS to 190 MPa for AZ61 and to 250 MPa for AZX611. The grain size of strip-processed AZ61 and AZX611 alloys was 3 μm regardless of the strip-processing speed. The grain size normally coarsens with increasing strip-processing speed; however, unlike the case of multipass strip processing, the rolling speed has no apparent effect on the crystal texture in the one-pass TRC process because of the effects of processing heating. The Al–Ca

compounds that form at the grain boundaries in TRC AZX611 alloy reorient parallel to the rolling direction after strip processing. On the other hand, the microstructure of processed AZX612 alloy is similar to that of AZ61 and AZX611 alloys, as described above, but the tensile properties are independent of the strip-processing speed. The area ratio of Al–Ca compounds in TRC AZX611 alloy is 7.1%. However, in AZX612 alloy, this value increases to 18.1%, and the decrease in strength for strips processed with a large reduction ratio is small. Furthermore, as shown in Figure 13, Al–Ca compounds dispersed in the Mg phase inhibit the growth of Mg phase grains. Solution treatment or homogenizing treatment is typically necessary when Al–Ca compounds develop. It is easier to strip process AZX612 alloy than gravity-cast material, and the dispersion of compounds is the dominant factor in plastic deformation. Figure 14 shows the relationship between the annealing temperature and the grain size when a material strip processed at a roll speed of 5 m min^{-1} is annealed for one hour; it also shows the OM microstructure of material annealed for one hour at 400 °C. Crystal grains of AZ61 alloy grew rapidly at an annealing temperature of 350 °C. However, as the amount of added Ca was increased, the ultimate grain size was 10 μm in AZX611 alloy and 7 μm in AZX612 alloy, even when the annealing temperature was increased. There are no compounds that inhibit grain growth in AZ61, whereas Al–Ca compounds inhibit grain growth in AZX611 and AZX612 alloys. The area ratio of Al–Ca compounds is higher in AZX612, and large amounts of dispersion into the Mg phase after strip processing effectively inhibit grain growth. These results suggest that adding more Ca results in an improvement in thermal resistivity, and agrees with a report on improvement of creep-resistance properties [14].

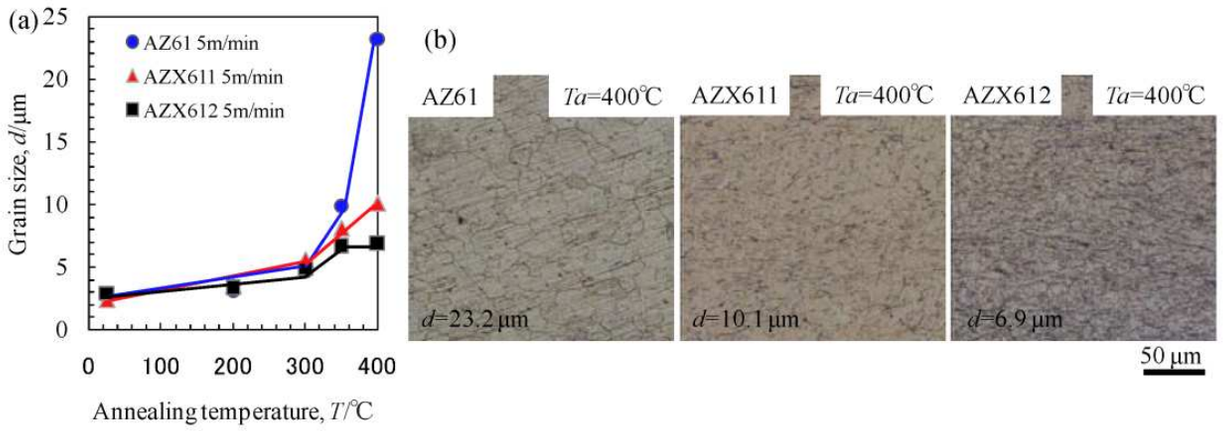

Figure 14. (a) Relationship between the annealing temperature and the grain size for AZ61, AZX611, and AZX612 single-pass-rolled materials. Annealing was performed at 200, 300, 350, or 400 °C for one hour. (b) Optical micrographs of materials annealed at 400 °C for one hour.

http://dx.doi.org/10.5772/58940

The TRC material prepared in this research had an equiaxial microstructure, permitting a large rolling reduction of about 65% per pass. For Mg alloys that form Al–Ca compounds on addition of Ca, resulting in deterioration of the plastic-deformation performance, twin-roll casting is an effective processing method, although it is limited to the manufacture of sheet materials. With regard to the microstructure after strip processing, although the internal microstructure of the TRC material varied with the twin-roll casting conditions, in no case was there mixing of grain size in the internal microstructure, that is, there was no mixing of the coarse microstructure at the surface of the sheets with the refined internal microstructure. No solution treatment or microstructure homogenization treatment is carried out after twin-roll casting of AZ61 alloy; as a result, the β-phase remains elongated along the rolling direction.

3.4. Corrosion behavior of rolled magnesium alloys

There are many reports on the corrosion resistance of generic AZ-type Mg alloys, but few reports on those of noncombustible Ca-containing Mg alloys. We therefore examined the corrosion properties of such alloys.

Samples of TRC Mg–3Al–1Zn–1Ca (AZX311), Mg–6Al–1Zn–1Ca (AZX611), and Mg–10Al–0.2Mn–1Ca (AMX1001) alloy sheets were warm-forged from a thickness of 3 mm to 1 mm. Although TRC materials have good strip-processing properties, to avoid mixing of grains in the internal microstructure as a result of strip processing, three-pass processing was employed with a roll speed of 10 m min^{-1}, a roll-surface temperature of 200 °C, and a specimen temperature of 250 °C. Reheating for 1 min was carried out between each pass, and the specimens were water cooled at the end of the process. Immersion tests were carried out in 5% aqueous NaCl at a constant temperature of 25 °C for up to 120 hours. Changes in weight and in surface microstructure were observed. After immersion, the material was prepared for examination by means of surface polishing, degreasing with acetone, and cutting into samples 20 mm long by 20 mm wide.

The average grain size of AZX311, AZX611, and AMX1001 strip-rolled alloys was 3.5 μm, and refined equiaxial grains and some elongated microstructure that had not recrystallized remained. The YS of all the alloys was around 330 MPa, the UTS was 350 MPa, and the elongation was 5% [3, 11, 35]. The relationship between the change in weight and the immersion time shown in Figure 15(a) indicates that, for noncombustible Mg alloy containing 1 mass % of Ca, an increase in the Al content reduces the change in weight with increasing immersion time in a manner similar to that shown by generic AZ-type Mg alloys. The weight monotonously decreased for immersion times of up to 100 hours, and then changed quadratically regardless of the Al content. In the region where the weight decreased monotonously, filiform corrosion and partial pitting was observed at the sheet surface, as shown in the OM microstructure of Figure 15(b); however, these processes did not lead to significant weight losses because the crystal microstructure was refined. On the other hand, filiform corrosion and pitting per unit area increased with time, and these propagated and combined, leading to pitting of the entire surface of the sheet and a significant reduction in weight. Refined disper-

sion of Ca or Al–Ca compounds in the more-refined Mg phase as a result of casting and strip processing does not result in significant reduction in the corrosion resistance caused by intermetallic compounds if the amount of added Ca is only 1 mass%.

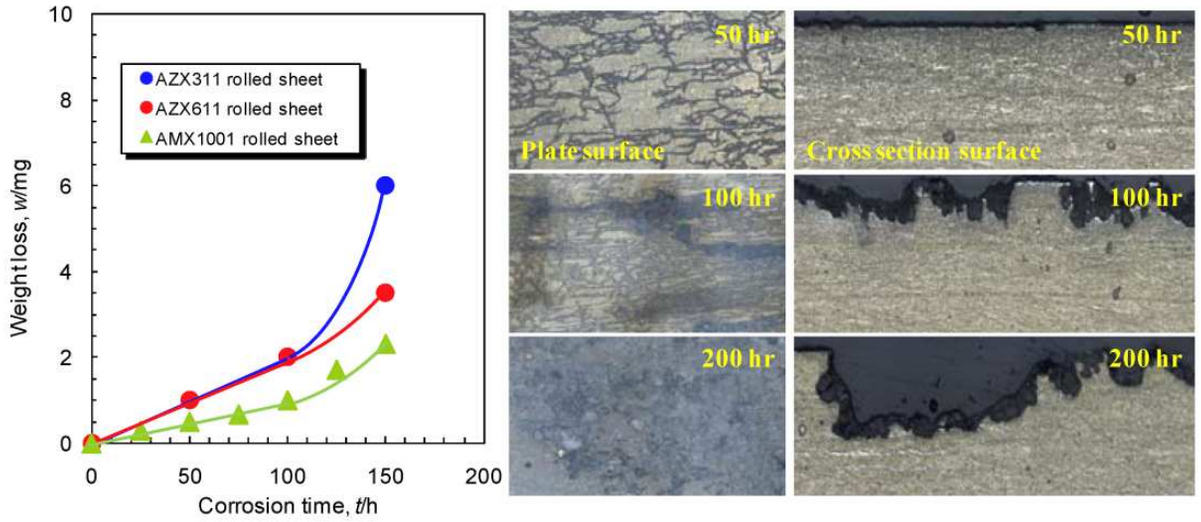

Figure 15. (a) Relationship between weight loss and immersion time for AZX311, AZX611, and AMX1001 rolled materials. (b) Optical micrographs of plate surfaces after immersion tests in an 5% aqueous NaCl solution.

4. Summary

In this present study, we investigated on the effects of melt purification during melting before twin-roll casting on the production of sheet metals. Using an Ar gas melting atmosphere prevented combustion at ingot alloy surface, and the amount of slug and oxide inclusions in the cast material decreased. By reducing the cooling rate from that of fast solidification at over 100 °C s^{-1}, characteristic of twin-roll casting, to around 50 °C s^{-1}, samples of TRC Mg alloy material 300 mm wide by 5 m long that form intermetallic compounds can be prepared without cracking. The grain size at the surface of the TRC material is about 2.5 times larger than that in the interior. As the Ca content increases, the crystal grain size becomes smaller and the area ratio of intermetallic compounds increases. The use of TRC materials instead of cast materials with a dendrite microstructure and/or coarse grains results in good strip-processing performance as a result of random crystal orientation, formation of a refined microstructure, and refined dispersion of Al–Ca compounds. Refined dispersion of Ca or Al–Ca compounds in the more-refined Mg phase as a result of casting and strip processing does not result in significant reduction in the corrosion resistance.

http://dx.doi.org/10.5772/58940

Author details

Masafumi Noda[1], Tomomi Ito[2], Yoshio Gonda[2], Hisashi Mori[3] and Kunio Funami[1]

*Address all correspondence to: mk-noda@s7.dion.ne.jp

1 Department of Mechanical Science and Engineering, Chiba Institute of Technology, Narashino, Chiba, Japan

2 Magnesium Division, Gonda Metal Industry Co., Ltd., Sagamihara, Kanagawa, Japan

3 Railway Technical Research Institute, Kokubunji, Tokyo, Japan

References

[1] Kamado S, Koike J, Kondoh K, Kawamura Y. Magnesium Research Trend in Japan. Materials Science Forum 2003; 419–422 21–34.

[2] Luo AA. Recent Magnesium Alloy Development for Automotive Powertrain Applications. Materials Science Forum 2003; 419–422 57–66.

[3] Mori H, Fujino K, Kurita K, Chino Y, Saito N, Noda M, Komai H, Obara H. Application of the Flame Retardant Magnesium Alloy to High Speed Rail Vehicles. Materia Japan 2013; 52(10) 484–490 (in Japanese). DOI 10.2320/material.52.484.

[4] Chen FK, Huang TB, Chang CK. Deep Drawing of Square Cups with Magnesium Alloy AZ31 Sheets. International Journal of Machine Tools and Manufacture 2003; 43(15) 1553–1559.

[5] Noda M, Matsumoto R, Kawamura Y. Forging Induces Changes in the Formability and Microstructure of Extruded $Mg_{96}Zn_2Y_2$ Alloy with a Long Period Stacking Order Phase. Materials Science and Engineering A 2013; 563 (15) 21–27.

[6] Yoo MH. Slip, Twinning, and Fracture in Hexagonal Close-Packed Metals. Metallurgical Transactions A 1981; 12(3) 409–418.

[7] Wang Y, Lui G, Fan Z. Microstructural Evolution of Rheo-Diecast AZ91D Magnesium Alloy During Heat Treatment. Acta Materialia 2006; 54(3) 689–699.

[8] Czerwinski, F., Magnesium Injection Molding,. New York, Springer Verlag, 2008; 19-21.

[9] Paliwal M, Jung IH. The Evolution of the Growth Morphology in Mg–Al Alloys Depending on the Cooling Rate During Solidification. Acta Materialia 2013; 61(13) 4848–4860.

[10] For examples, see: Kojima Y, Aizawa T, Kamado S., editors. Magnesium Alloys 2000: Volumes 350–351, Materials Science Forum, Trans Tech Publications, DOI: 10.4028/www.scientific.net/MSF.350-351.

[11] Noda M, Sakai N, Funami K, Mori H, Fujino K. High Strength and Grain Refinement of Mg-3Al-1Zn-1Ca Alloy by Rolling. Journal of the Japan Society for Technology of Plasticity 2013; 54(625) 143–147.

[12] Kawamura Y, Hayashi K, Inoue A, Masumoto T. Rapidly Solidified Powder Metallurgy $Mg_{97}Zn_1Y_2$ Alloys with Excellent Tensile Yield Strength above 600 MPa. Materials Transactions 2001; 42(7) 1172–1176.

[13] Jian WW, Cheng GM, Xu WZ, Yuan H, Tsai MH, Wang QD, Koch CC, Zhu YT, Mathaudhu SN. Ultrastrong Mg Alloy via Nano-Spaced Stacking Faults. Materials Research Letters 2013; 1(2) 61–66.

[14] Maruyama K, Suzuki M, Sato H. Creep Strength of Magnesium-Based Alloys. Metallurgical and Materials Transactions A 2002; 33(13) 875–882.

[15] Noda M, Kawamura Y, Mayama T, Funami K (2012), Thermal Stability and Mechanical Properties of Extruded Mg-Zn-Y Alloys with a Long-Period Stacking Order Phase and Plastic Deformation. In: Monteiro WA (ed.) New Features on Magnesium Alloys, Rijeka, InTech, 2012; DOI: 10.5772/48202.

[16] Matsumoto R, Osakada K. Effect of Heat Treatment on Forgeability of AZ31 Magnesium Alloy. Journal of Japan Institute of Light Metals 2007; 57(7) 274–279.

[17] Chino Y, Mabuchi M, Kishihara R, Hosokawa H, Yamada Y, Wen C, Shimojima K, Iwasaki H. Mechanical Properties and Press Formability at Room Temperature of AZ31 Mg Alloy Processed by Single Roller Drive Rolling. Materials Transactions 2002; 43(10) 2554–2560.

[18] Xu SW, Oh-ishi K, Sunohara H, Kamado S. Extruded Mg–Zn–Ca–Mn Alloys with Low Yield Anisotropy. Materials Science and Engineering A 2012; 558 356–365.

[19] Yim CD, You BS, Lee JS, Kim WC. Optimization of Hot Rolling Process of Gravity Cast AZ31-xCa (x=0–2.0 mass%) Alloys. Materials Transactions 2004; 45(10) 3018–3022.

[20] Furui M, Ebata Y, Yamada H, Ikeno S, Sakakibara K, Saikawa S. Grain Boundary and Intragranular Reactions During Aging in Mg-Al System Alloys Poured into Sand and Iron Molds. Materials Transactions 2011; 52(3) 285–291.

[21] Ion SE, Humphreys FJ, White SH. Dynamic Recrystallisation and the Development of Microstructure During the High Temperature Deformation of Magnesium. Acta Metallurgica 1982; 30(10) 1909–1919.

[22] Myshlyaev MM, McQueen HJ, Mwembela A, Konopleva E. Twining, Dynamic Recovery and Recrystallization in Hot Worked Mg–Al–Zn Alloy. Materials Science and Engineering A 2002; 337(1–2) 121–133.

[23] Watanabe H, Ishikawa K. Effect of Texture on High Temperature Deformation Behavior at High Strain Rates in a Mg–3Al–1Zn Alloy. Materials Science and Engineering A 2009; 523(1–2) 304–311.

[24] Agnew SR, Yoo MH, Tomé CN. Application of Texture Simulation to Understanding Mechanical Behavior of Mg and Solid Solution Alloys Containing Li or Y. Acta Materialia 2001; 49(20) 4277–4289.

[25] Akiyama S, Ueno H, Sakamoto M, Hirai H, Kitahara A. Development of Noncombustible Magnesium Alloys. Materia Japan 2000; 39(1) 72–74 (in Japanese).

[26] Kawamura Y, Yamasaki M. Ignition temperature and mechanical properties of nonflammable magnesium alloys with high strength. In: Collected abstracts of the 2013 Spring meeting of Japan Institute of Light Metals, 18–19 May 2013, University of Toyama, Japan. Japan Institute of Light Metals, Tokyo; 131–132.

[27] Czerwinski. F., Controlling the ignitions and flammability of magnesium for aerospace applications. Corrosion Science 2014; 86 1-16.

[28] Prasad A, Shi Z, Atrens A. Influence of Al and Y on the Ignition and Flammability of Mg Alloys. Corrosion Science 2012; 55 153–163.

[29] Haga T, Takahashi K. Casting of Composite Strip Using a Twin Roll Caster. Journal of Materials Processing Technology 2004; 157–158 701–705.

[30] Park SS, Bae GT, Kang DH, Jung IH, Shin KS, Kim NJ. Microstructure and Tensile Properties of Twin Roll Cast Mg–Zn–Mn–Al Alloys. Scripta Materialia 2007; 57(9) 793–796.

[31] Jiang B, Liu W, Qiu D, Zhang MX, Pan F. Grain Refinement of Ca Addition in a Twin Roll Cast Mg–3Al–1Zn Alloy. Materials Chemistry and Physics 2012; 133(2–3) 611–616.

[32] Zhao Hu, Li P, He L. Microstructure and Mechanical Properties of an Asymmetric Twin Roll Cast AZ31 Magnesium Alloy Strip. Journal of Materials Processing Technology 2012; 212(8) 1670–1675.

[33] Savage SJ, Froes FH. Production of Rapidly Solidified Metals and Alloys. JOM: The Journal of the Minerals, Metals & Materials Society 1984; 36(4) 20–33.

[34] Watari H, Davy K, Rasgado MT, Haga T, Izawa S. Semi-solid manufacturing process of magnesium alloys by twin-roll casting. Journal of Materials Processing Technology 2004; 155–156 1662–1667.

[35] Ito T, Noda M, Mori H, Gonda Y, Fukuda Y, Yanagihara S. Effect of Antigravity Suction Casting Parameters on Microstructure and Mechanical Properties of Mg–10Al–0.2Mn–1Ca Cast Alloy. Materials Transactions 2014; 55(8) 1184-1189

IntechOpen